JOURNAL OF GUIDANCE, CONTROL, AND DYNAMICS
Vol. 34, No. 3, May–June 2011

Engineering Notes

Dynamic Systems Approach to the Lander Descent Problem

Y. H. Shang,* K. Uldall Kristiansen,† and P. L. Palmer‡
University of Surrey,
Guildford, England GU2 7XH, United Kingdom

DOI: 10.2514/1.52964

Introduction

THE gravity turn landing scheme was originally developed for the 1966–1968 Lunar Surveyor landing mission [1]. Since then it has been applied in many landing missions such as the Viking Lander and Mars Polar Lander [2]. The descent method has the advantage of being near fuel optimal while guaranteeing a vertical landing [3,4]. However, the method requires a control system that can apply the thrust antiparallel to the instantaneous velocity vector for the entire descent.

This Note focuses on the dynamic aspects of the landing scheme. The immediate problem here is to solve for the control that takes the lander from a circular, or near-circular, initial parking orbit to the surface of the planet with zero final relative velocity and zero flight-path angle. In the past, this problem has been studied primarily through various assumptions. The studies can generally be divided into two groups corresponding to two different assumptions: 1) descent from low altitude and 2) a flat planet. In [3,5] both assumptions are considered and compared for the case of a constant thrust-to-weight ratio. Using the first assumption, the authors argue for the validity of approximating the full nonlinear gravity with a constant gravity while maintaining, or at least an approximation of, the Coriolis force. This way, one of the equations decouple from the remaining two equations, which can then be solved by quadrature. Using the second assumption (see also [4,6]), both the gravity gradient and the Coriolis forces are neglected. This truncation can be solved analytically. In particular, the authors in [6] obtain analytical solutions with an inclusion of a quadratic air drag. It is shown that the effect of the drag is to increase the effective thrust–weight ratio so that the descent is completed with a lower thrust compared with the vacuum case.

In this Note, the problem is considered without any assumptions on the gravity and the Coriolis forces. The approach undertaken here is also more geometric and includes an initial qualitative analysis. Furthermore, a closed-form solution is derived for the case of a controller that depends upon the flight-path angle. Finally, a numerical analysis is provided for the full problem with constant thrust to mass ratio. Through an appropriate choice of scaling the numerical solution of the required control is presented through a single planar plot, regardless of the parameters of the problem.

Received 29 October 2010; revision received 10 December 2010; accepted for publication 10 December 2010.

*Ph.D. Student, Surrey Space Center; y.shang@surrey.ac.uk.
†Ph.D. Student, Department of Mathematics and Surrey Space Center; kristian.kristiansen@surrey.ac.uk.
‡Reader, Surrey Space Center; p.palmer@surrey.ac.uk. Member AIAA.

Model

To set up the controlled system, Kepler's equations in the plane

$$\ddot{x} = -\frac{\mu x}{|x|^3}, \qquad x \in \mathbb{R}^2\backslash\{0\}$$

in which μ is the gravitational constant of the planet, are first rewritten through the transformation $x \mapsto \tilde{x} = \mu x$, $t \mapsto \tilde{t} = \mu^2 t$ so that

$$\ddot{\tilde{x}} = -\frac{\tilde{x}}{|\tilde{x}|^3} \tag{1}$$

in which $\dot{()} = \frac{d}{d\tilde{t}}$. Henceforth, the tildes are dropped. Next, polar coordinates (ν, r) are introduced for x, $V = |\dot{x}|$ and ϕ is introduced as the angle between $\dot{x}$ and x:

$$x = re_\nu, \qquad v = Ve_{\nu+\pi-\phi}$$

Here, $e_\theta = (\cos\theta, \sin\theta)$ is a vector on the unit circle. See also Fig. 1. This transforms Eq. (1) into

$$\dot{r} = -V\cos\phi \tag{2}$$

$$\dot{V} = \frac{1}{r^2}\cos\phi \tag{3}$$

$$r\dot{\nu} = V\sin\phi \tag{4}$$

$$V\dot{\phi} = \left(\frac{V^2}{r} - \frac{1}{r^2}\right)\sin\phi \tag{5}$$

Notice that Eqs. (2), (3), and (5) are independent of ν and Eq. (4) therefore decouples. For the gravity turn landing scheme the constant thrust to mass control $u = \text{const.} < 0$ is applied in the direction of the velocity and hence only enters on the right-hand side of Eq. (3):

$$\dot{V} = \frac{1}{r^2}\cos\phi + u \tag{6}$$

The singularity in Eq. (5) is due to ϕ not being defined for $V = 0$. However, a singularity is inevitable in any coordinates since the control u is undefined for $V = 0$. Particularly, the system is only defined for $V > 0$. By undoing the preceding μ-dependent scaling, it may be realized that the dimensional control is given by $\mu^3 u$.

Attention is restricted to initial conditions that are compatible with a circular orbit: $r(0) = r_0$, $V(0) = r_0^{-1/2}$, and $\phi(0) = \pi/2$. The aim is to obtain a control $u = u(r_0, r_f)$ such that $\lim_{t\to t_\infty} r(t) = r_f > 0$, $\lim_{t\to t_\infty} V(t) = 0$, and $\lim_{t\to t_\infty} \phi(t) = 0$ in which t_∞ is time of descent.

There exists a nonlinear change of time $t \mapsto \tau$ such that Eqs. (2), (5), and (6) become

$$r' = -V^2\cos\phi \tag{7}$$

$$V' = V\left(\frac{1}{r^2}\cos\phi + u\right) \tag{8}$$

$$\phi' = \left(\frac{V^2}{r} - \frac{1}{r^2}\right)\sin\phi \tag{9}$$

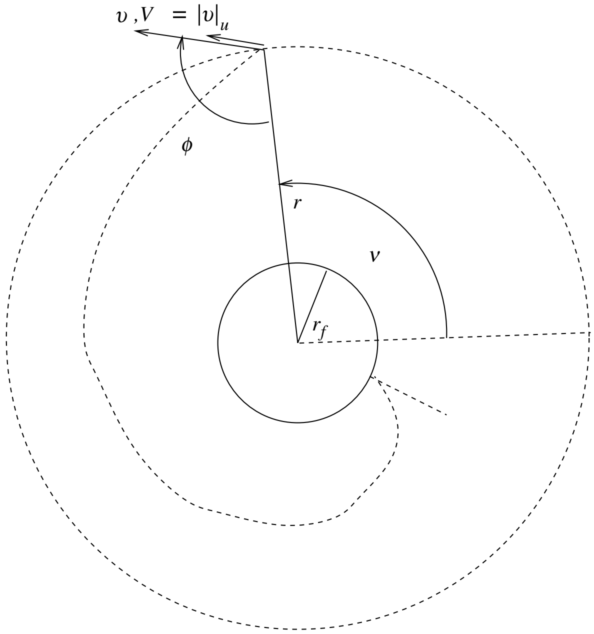

Fig. 1 A schematic definition of the variables used in the analysis: (r, ν) are polar coordinates of the satellite position $x \in \mathbb{R}^2$, V is the norm of the velocity, and ϕ is the angle between $\dot{x}$ and x.

with $()' = \frac{d}{d\tau}$. In fact, $t = t(\tau)$ solves

$$t' = V$$

Within the system of Eqs. (7–9), the singularity at $V = 0$ is no longer explicit. It is implicit in the sense that the transformation is only invertible for $V \neq 0$ and in particular the system of Eqs. (2), (5), and (6) is only equivalent with the system of Eqs. (7–9) for $V \neq 0$. In the system of Eqs. (7–9), $V = 0$ corresponds to zeros of the right-hand sides of Eqs. (7) and (8). The sets $M = \{V = 0, \phi = 0\}$ and $\{V = 0, \phi = \pi\}$ are sets of equilibria parametrized by r. Attention is restricted to M. A linearization in the normal direction ((V, ϕ) plane) of M gives

$$\delta V' = \delta V\left(\frac{1}{r^2} + u\right), \qquad \delta\phi' = -\frac{1}{r^2}\delta\phi$$

Clearly, if $u < -\frac{1}{r^2}$, then M is stable with a three-dimensional stable manifold:

$$W_s(M) = \{\text{set of trajectories that approach } M \text{ asymptotically}\}$$

If $u = \frac{1}{r^2}$, then M has one neutral direction (V direction) and one stable direction (ϕ direction). The points of M are all singular points of Eqs. (2), (3), and (5), but the stable manifolds are not and therefore exists as solutions to the original equations.

For the descent of the lander, the aim is therefore to choose initial conditions on the stable manifold $W_s(M)$ with base point $r = r_f$, in which r_f is the surface radius of the planet, so that $(r, V, \phi)(t) \to M$ with $r \to r_f$ for $t \to t_\infty$.

The existence of a stable manifold M does not mean that regardless of the control $u < 0$ all trajectories initially on a circular orbit approach M. In other words, not all of these trajectories live on $W_s(M)$. For example, if $|u|$ is not large enough then trajectories may "bounce" near the surface of the planet. This will, however, only occur if $u > -\frac{1}{r_f}$. Such a bounce may be constructed by assuming that the solution initially starts from a circular orbit with radius r_0 and that the control is sufficiently close to $-\frac{1}{r_0^2}$ while satisfying $u < -\frac{1}{r_0^2}$. Then, $\dot{V}$ vanishes at some time $t = t_0$ with $\phi(t_0) > 0$ and $V(t_0) > 0$. In particular, from Eq. (6),

$$\ddot{V}(t_0) = \frac{(3c(t_0)^2 - 1)V(t_0)}{r(t_0)^3} + \frac{1 - c(t_0)^2}{V(t_0)r(t_0)^4}$$

in which $c(t) = \cos\phi(t)$. Certainly, if $c(t_0) \in (1/3, 1)$ then $\ddot{V}(t_0) > 0$ and V starts to increase. When V increases, then ϕ will eventually also increase [Eq. (9)].

Analytical Approach

In this section, an analytical expression for the required control is derived when the control has the particular form $u = \tilde{u}\cos\phi$, $\tilde{u} < 0$ constant. The preceding analysis of M is still applicable. On the other hand, with this controller the system has another family N of unstable equilibria:

$$N = \{V = r^{-1/2}, \phi = \pi/2\}$$

parametrized by r, which correspond to the initial circular orbits. Geometrically, our boundary value problem can therefore be stated as follows: obtain solutions connecting the two one-dimensional manifolds M and N in the three-dimensional space (r, V, ϕ). These connections are due to the intersections of the unstable manifold of N and the stable manifold of M.

When $u = \tilde{u}\cos\phi$, $\tilde{u} < 0$, then Eqs. (7–9) read

$$r' = -V^2\cos\phi \tag{10}$$

$$V' = V\left(\frac{1}{r^2} + \tilde{u}\right)\cos\phi \tag{11}$$

$$\phi' = \left(\frac{V^2}{r} - \frac{1}{r^2}\right)\sin\phi \tag{12}$$

This controller is henceforth referred to as the angle-dependent controller. Here, ϕ can be eliminated from the first two equations by, basically, dividing Eqs. (10) and (11):

$$\frac{dr}{dV} = -\frac{V}{r^{-2} + \tilde{u}}$$

This equation, in terms of $r = r(V)$ with $r(V = r_0^{-1/2}) = r_0$, solves to

$$r(V) = \frac{1}{2}\left(r_0 - \frac{1}{2\tilde{u}r_0}\right) - \frac{V^2}{4\tilde{u}} - \sqrt{\left(\frac{V^2}{4\tilde{u}}\right)^2 - \left(\frac{V^2}{4\tilde{u}}\right)\left(r_0 - \frac{1}{2\tilde{u}r_0}\right) + \frac{1}{4}\left(r_0 - \frac{1}{2\tilde{u}r_0}\right)^2 + \frac{1}{\tilde{u}}}$$

when $\tilde{u} < -r_0^{-2}$. Particularly, for $V = 0$,

$$r(0) = \frac{1}{2}\left(r_0 - \frac{1}{2\tilde{u}r_0}\right) - \sqrt{\frac{1}{4}\left(r_0 - \frac{1}{2\tilde{u}r_0}\right)^2 + \frac{1}{\tilde{u}}}$$

Setting $r(0) = r_f$ the aim is to solve for $\tilde{u}$. This can be done for $\gamma \equiv \frac{r_0}{r_f} \in (1, 1 + 1/\sqrt{2})$ giving

$$\tilde{u} = -\frac{2r_0 - r_f}{2r_f r_0(r_0 - r_f)} = -\frac{1}{2r_f^2}\frac{2\gamma - 1}{\gamma(\gamma - 1)}$$

The upper bound for $\gamma = \bar{\gamma} = 1 + 1/\sqrt{2} \approx 1.70$ corresponds to $\tilde{u} = -\frac{1}{r_f^2}$ for which the time of descent t_∞ becomes infinite. Indeed, it follows that $\dot{V}_{\gamma=\bar{\gamma}} \to 0^-$. At the other extreme, $|\tilde{u}| \to \infty$ for $\gamma = \frac{r_0}{r_f} \to 1$. The control has to be of infinite magnitude to instantaneously change the magnitude of the velocity and its direction.

The acceleration [Eq. (6)] at the time of descent is

$$\dot{V}(t_\infty) = \frac{1}{r_f^2} + \tilde{u} = \frac{1}{r_f^2}\left(1 - \frac{2\gamma - 1}{2\gamma(\gamma - 1)}\right) < 0, \quad \text{for } 1 < \gamma < \bar{\gamma} \tag{13}$$

is important in the design of the controller. In particular, it is expected that the higher value of this acceleration the shorter is the landing

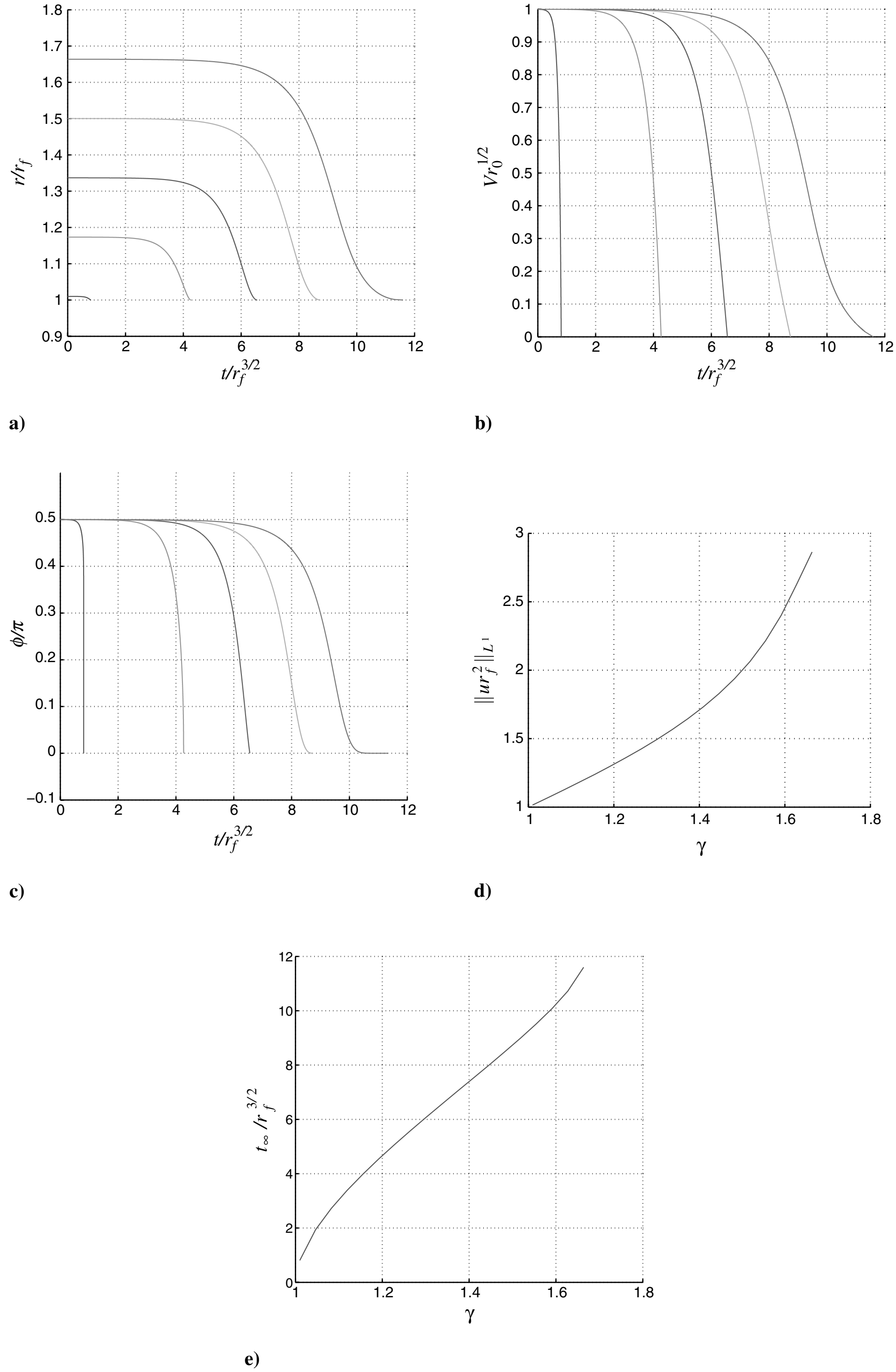

Fig. 2 The solutions: a) $r(t)$, b) $V(t)$, and c) $\phi(t)$ for five equidistant γ values between 1.01 and 1.69 for the angle-dependent controller, and d) consumed control $\|u\|_{L^1}$ and e) time of descent t_∞ as a function of γ.

time. Later on, it shall be shown that this is indeed the case (Fig. 2e). On the other hand, a large change in the velocity is not desired near the surface due to the possibility of uncertainties in the surface radius. A lower acceleration is, however, associated with longer landing time and more control. From Eq. (13), it is realized that $\dot{V}(t_\infty)$ is monotonically increasing as a function of γ: $\frac{\partial}{\partial\gamma}\dot{V}(t_\infty) > 0$, with $\dot{V}(t_\infty) \to -\infty$ and $\dot{V}(t_\infty) \to 0$ for $\gamma \to 1^+$ and $\bar{\gamma}$, respectively, from below.

In Figs. 2a–2c the solutions $r(t)$, $V(t)$ and $\phi(t)$, respectively, are shown for 5 equidistant γ values between 1.01 and 1.69. In Figs. 2d and 2e, the consumed control $\|u\|_{L^1} = \int_0^{t_\infty} |\tilde{u}\cos\phi(t)|\,\mathrm{d}t$ and the time of descent t_∞ are shown as functions of γ. It is obvious that $r \to r_f$ while $V, \phi \to 0$. The control and the time of descent increase monotonically as γ increases.

Numerical Approach

Motivated by the analytical approach just described, the case of constant thrust $u < 0$ is now considered. Here, it is the aim to obtain a relation between ur_f^2 and $\gamma = \frac{r_0}{r_f}$ numerically. The existence of such a unique relation is due to invariance of the equations to the following scaling. Let $r \mapsto \tilde{r} = \frac{r}{r^*}$, $V \mapsto \tilde{V} = Vr^{*1/2}$, $\phi \mapsto \tilde{\phi} = \phi$, $t \mapsto \tilde{t} = r^{*-3/2}t$, $u \mapsto \tilde{u} = ur^{*2}$ for any $r^* \neq 0$ then

$$\dot{\tilde{r}} = -\tilde{V}\cos\tilde{\phi}, \qquad \dot{\tilde{V}} = \frac{1}{\tilde{r}^2}\cos\tilde{\phi} + \tilde{u}, \qquad \tilde{V}\,\dot{\tilde{\phi}} = \left(\frac{\tilde{V}^2}{\tilde{r}} - \frac{1}{\tilde{r}^2}\right)\sin\tilde{\phi}$$

in which $\dot{()} = \mathrm{d}/\mathrm{d}\tilde{t}$. Particularly, this means that attention may be restricted to $r(0) = 1$. This way, our numerical solution of the required control can be presented through a single planar plot (Fig. 3d), regardless of the parameters of the problem.

In Figs. 3a–3c, the solutions $r(t)$, $V(t)$ and $\phi(t)$, respectively, are shown for $\gamma = 1.16$, 1.12, 1.08, 1.04, 1.02. In Figs. 3d and 3e, the nondimensionalized control ur_f^2 and the time of descent $r_f^{3/2}t_\infty$, respectively, are shown as functions of γ together with the corresponding plots (the dotted lines) from Fig. 2. It should be noted that it was not possible to do continuation for γ values exceeding $\gamma = \bar{\gamma} \approx 1.162$. Beyond this value $\dot{V}$ vanishes before $V = 0$ and the solutions bounce, as described, just before reaching the surface of the planet. This upper bound on γ is substantially less than $1 + 1/\sqrt{2}$ for the angle-dependent control considered in the previous section. This is to be expected as V increases much faster, in fact $\dot{V}$ is for the

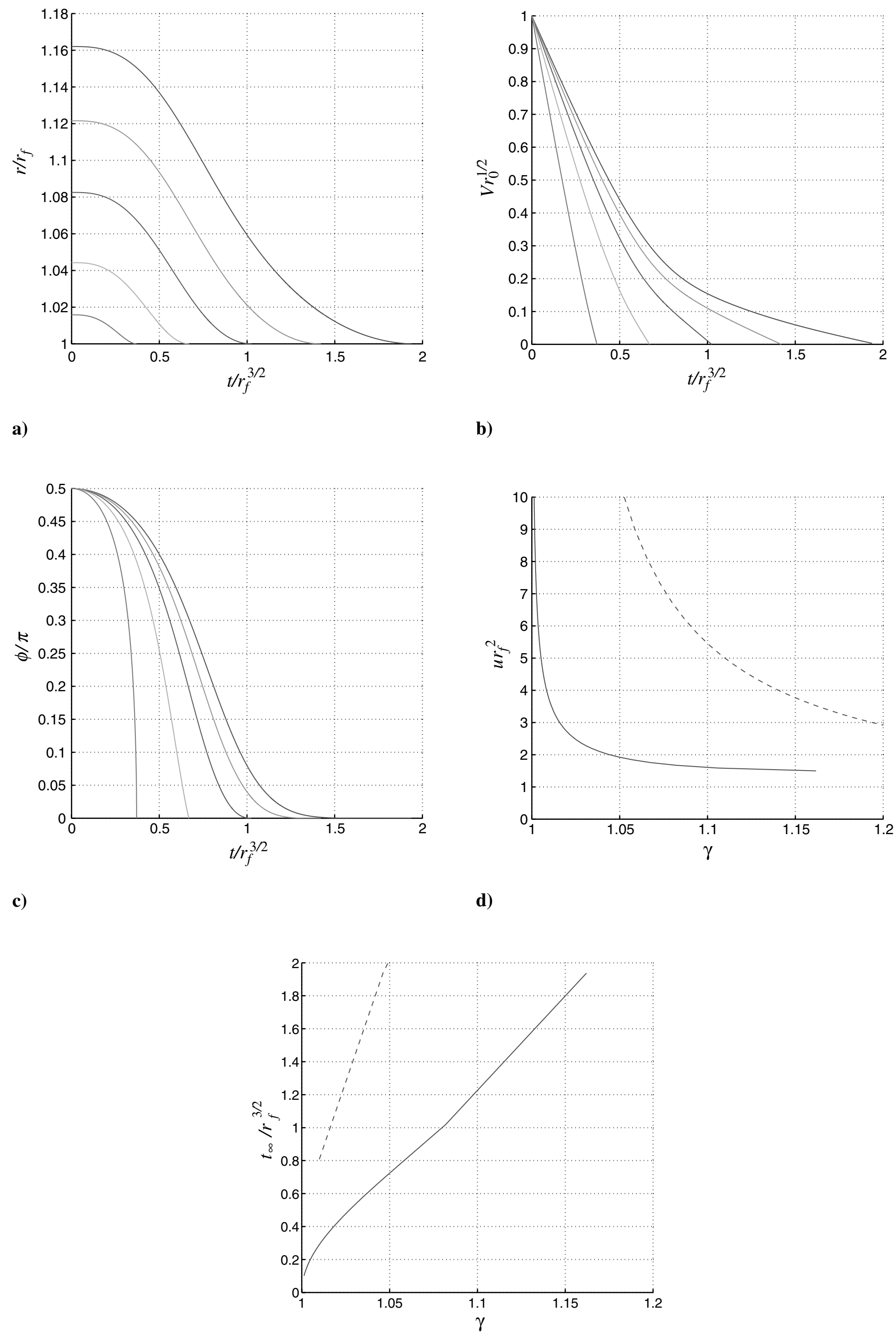

Fig. 3 The solutions: $r(t)$, $V(t)$, $\phi(t)$ for $\gamma = 1.16$, 1.12, 1.08, 1.04, 1.02: d) required control ur_f^2 and e) time of descent t_∞ are plotted as a function of γ together with the corresponding plots (the dotted lines) from Fig. 2. Notice that the lower values of γ correspond to shorter times of descent.

constant thrust to mass ratio controller at the beginning of the descent well approximated by u [Eq. (8)] with $\phi \approx \pi/2$ and Fig. 3b. This is not the case for the angle-dependent controller in which $\dot{V}$ decreases very slowly initially (see Fig. 2b).

From Figs. 3d and 3e, it is concluded that for a given γ the constant thrust uses less time and less control than the angle-dependent controller. For those reasons the angle-dependent controller is perhaps of limited practical interest. Furthermore, an angle-dependent controller obviously adds further complexity to the system as, in practice, it is to be used in conjunction with a sensor measuring the flight-path angle. However, the maximal radius of the initial circular orbit can be chosen much larger than compared with the constant thrust to mass ratio controller.

Conclusions

This Note considers the descent of a lander from an initial circular orbit to the surface of a planet using gravity turn. By choosing a controller depending upon the flight-path angle, an analytical expression was obtained for the required control as a function of the initial radius and the radius of the planet. With this controller, the system was also shown to possess an interesting geometry. Indeed, the initial circular orbits and, through a proper scaling, the final states at the surface of the planet were shown to be equilibria of the system. The solutions to the problem were then geometrically interpreted as heteroclinic connections between these equilibria. The constant thrust-to-mass controller was treated numerically, and through a proper scaling the required control for a given initial and final radius through one single planar plot was determined. This controller was for a given initial altitude shown to outperform the angle-dependent controller both in terms of the used thrust but also in terms of the time of descent. However, for the constant thrust-to-weight controller it was numerically concluded that the ratio between the radius of the initial circular orbit to the radius of the planet could not exceed ≈ 1.162. For the angle-dependent controller, this maximum allowable ratio was larger: $1 + 1/\sqrt{2} \approx 1.70$. The fact that the constant thrust controller was only applicable for relative low altitudes provides, in some sense, a global justification of the approximation of constant gravity used throughout the literature.

Acknowledgment

K. Uldall Kristiansen was supported by European Union funding for the Marie Curie Research Training Network AstroNet (contract number MRTN-CT-2006-035151).

References

[1] Alemany, K., Wells, G., Theisinger, J., Clark, I., and Braun, R., "Mars Entry, Descent, and Landing Parametric Sizing and Design Space Visualization Trades," AIAA Astrodynamics Specialist Conference, Keystone, CO, AIAA Paper 2006-6022, Aug. 2006.

[2] Thurman, S. W., "Surveyor Spacecraft Automatic Landing System," 27th Annual AAS Guidance and Control Conference, Breckenridge, CO, AAS Paper 04-062, 4–8 Feb. 2004.

[3] McInnes, C. R., "Gravity-Turn Descent from Low Circular Orbit Conditions," *Journal of Guidance, Control, and Dynamics*, Vol. 26, No. 1, 2003, pp. 183–185.
doi:10.2514/2.5033

[4] Cheng, R. K., Meredith, C. M., and Conrad, D. A., "Design Considerations for Surveyor Guidance," *Journal of Spacecraft and Rockets*, Vol. 3, No. 11, 1966, pp. 1569–1576.
doi:10.2514/3.28709

[5] Citron, S. J., Dunin, S. E., and Meissinger, H. F., "A Terminal Guidance Technique for Lunar Landing," *AIAA Journal*, Vol. 2, No. 3, 1964, pp. 503–509.
doi:10.2514/3.2362

[6] McInnes, C. R., "Gravity Turn Descent with Quadratic Air Drag," *Journal of Guidance, Control, and Dynamics*, Vol. 20, No. 2, 1997, pp. 393–394.
doi:10.2514/2.4052